

Diffusion Mechanisms and Capture Radii in Silicon

K. M. Beardmore*, W. Windl**, B. P. Haley***, and N. Grønbech-Jensen****

* Motorola Labs, Los Alamos, NM, USA, Keith.Beamore@Motorola.com

** The Ohio State University, Columbus, OH, USA, windl.1@osu.edu

*** University of California, Davis, CA, USA, bphaley@ucdavis.edu

**** University of California, Davis, CA, USA, ngjensen@ucdavis.edu

ABSTRACT

We have calculated the capture radii for several defect pairs, consisting of dopants and point defects (interstitials I and vacancies V, in silicon. Interaction potentials for I-V, I-B, P-V, and As-V were calculated using the VASP *ab initio* package. These potentials were then input into kinetic lattice Monte Carlo simulations in order to determine capture radii. We use and compare two Monte Carlo simulators, LAMOCA from Boston University and McMot, a code recently developed by ourselves. We find that capture radii are highly dependent upon the extent of the interaction allowed within the KLMC code. Calculated capture radii are considerably larger than those typically used in diffusion modeling.

Keywords: silicon, diffusion, KLMC, *ab initio*, dopant

1 INTRODUCTION

The standard method of doping silicon to modify its electrical properties for micro-electronics production is to introduce dopants via ion implantation and to heal the created damage by subsequent annealing. As electronic devices continue to shrink in size, the impact of physical modeling of implant and diffusion becomes increasingly important.

In continuum models as well as Monte Carlo simulations of diffusion which do not replicate the silicon lattice, a ‘capture radius’ describes reactions between defects which is not well characterized [1]. Only one previous study has tried to determine the capture radius quantitatively, while truncating defect-defect and defect-dopant interactions to sixth neighbors or less. [2] The *ab initio* calculations in the present work show that defect interactions are more long ranged, extending up to at least eighth-nearest neighbor distance.

Multiscale diffusion modeling includes computational methods ranging from first-principles calculations, classical molecular dynamics and kinetic lattice Monte Carlo (KLMC) simulations to numerically solved coupled continuum diffusion equations. In general, more detailed levels of simulation are used to calculate parameters used in coarser, but faster simulation schemes.

In the case of many dopants, a notable body of work exists at each of the different simulation levels. For As

diffusion, several first-principles studies [3]–[5] and some Monte-Carlo work on an intermediate simulation hierarchy level [2], [6], [7] exist besides traditional continuum modeling.

In the present work, capture radii in silicon are studied using KLMC simulation following the lines of Ref. [2]. For a quantitative evaluation, we calculated within density-functional theory the interaction potentials for several defect pairs and determined the most reasonable approximation for diffusion barriers between valleys of different energy, using the Vienna Ab initio Simulation Package (VASP) [8] and large simulation cells. Those results were used as input for the KLMC simulations to determine the capture radii for the defect pairs.

2 AB INITIO CALCULATIONS

Calculations were conducted with the efficient plane-wave ultra soft pseudopotential code VASP [8]. We used the generalized gradient approximation (GGA) for all calculations and an optimized lattice constant of 5.46 Å. We use a kinetic-energy cutoff of 208 eV and a 4³ Monkhorst-Pack **k**-point sampling.

Although all previous *ab-initio* work for vacancy-assisted diffusion in Si has been performed within 64-atom supercells, those have been shown several years ago to be of insufficient size for defects involving vacancies [9]. Therefore, we have calculated the interaction potentials between defects by structural relaxation in a 216 atom (3 × 3 × 3 unit cells) volume.

For each set of calculations, the two defects were placed in the cell, sampling all possible separation distances and orientations. Each initial configuration was relaxed and the energy and final configuration saved. For saddle point calculations, the nudged-elastic band method implemented in VASP has been used.

3 KINET. LATTICE MONTE CARLO

In the mesoscopic KLMC approach to diffusion, the simulation contains a model of a silicon lattice occupied by different particles (dopants, interstitials, silicon atoms) or unoccupied (vacancies). KLMC parameters such as interaction energies are obtained from experiment and *ab initio* MD calculations. The initial conditions for capture radii calculations involve two defects,

each either a vacancy, interstitial, or dopant randomly located on a 3D lattice in a given volume.

Depending on the interaction potential between a defect and another defect or dopant atom, the initial and final state of a mobile defect can have different energy levels, with no easy estimate for the saddle point energy in-between. Two approximations for such saddle points have been suggested in the past, involving the interaction energies and the diffusivity of an isolated vacancy in otherwise perfect Si.

The first approximates the barrier by the sum of the free-vacancy migration barrier, E_V^0 , to the energy of the higher-laying valley energy, $E_m = \max(E_i, E_f) + E_V^0$ [10]. The other suggests to add the free-vacancy migration energy to the average of the two valley energies, $E_m = (E_i + E_f) / 2 + E_V^0$ [6]. While the second approximation might sound more reasonable at first glance, it has the inherent danger to end up with a negative migration barrier in cases where $E_V^0 < (E_i + E_f) / 2$.

We find with a nudged-elastic band ab-initio calculation for vacancy diffusion from the 2nd to the 3rd-neighbor site that the saddlepoint is close to the energetically higher 3-rd neighbor site, and that its energy can be approximate well by the first approximation from above [10]. For vacancy diffusion from nearest to 2nd neighbor distance, however, we find a nearly vanishing diffusion barrier only slightly higher than the 2nd-neighbor energy, which is considerably smaller than 2nd-neighbor energy plus free-vacancy migration energy. Thus, the second approximation, which predicts *no* barrier in this case, seems to be the better approximation. Further work is necessary for a decisive result.

Since the diffusion step from nearest to 2nd neighbor is the most crucial one for vacancy-assisted dopant diffusion, we chose the second approximation in the present work. Lumping the migration energy into the lattice migration frequency, the hopping frequency is given by $\nu = \nu_m \exp[(E_i - E_f) / 2k_B T]$, where ν_m is the lattice migration frequency and $E_i - E_f$ the change in the system energy due to a transition.

All interactions used in determining system energies are assumed to be pairwise additive. The total binding energies are described by $E_x(i) = \sum_{y,j} E_{xy}(j) \times N_y(j)$, where $E_x(i)$ is the sum of all defect-defect binding energies for a point defect x at site i with other point defects y within the range of interaction. $N_y(j)$ is the number of y type defects at j th nearest neighbor to site i and $E_{xy}(j)$ is binding energy between x and y type defects at separation j . Defect-defect interaction energies were calculated using VASP as described above.

In continuum and off-lattice Monte Carlo models for dopant diffusion in silicon, the interaction between defects x and y is described by a rate constant,

$$k_{x,y} = 4\pi a_{x,y} (D_x + D_y), \quad (1)$$

where the capture radius $a_{x,y}$ is often chosen arbitrar-

ily. Since KLMC simulations explicitly include the silicon lattice structure, the capture rate $k_{x,y}$ can be calculated directly, based on the interaction potential obtained from *ab initio* calculations. Using initial random defect displacements within a simulation box of volume Ω , the capture rate is given by

$$k_{x,y} = \Omega / \langle \tau \rangle, \quad (2)$$

where $\langle \tau \rangle$ is the average capture time. Equation 1 is then inverted to give the capture radius.

Only hops to first nearest neighbor sites are considered. Periodic boundary conditions are assumed for all capture radius calculations. We have used two codes; initial calculations were conducted using the LAMOCA code from Boston University / University of Washington, which allows defect-defect interaction up to the sixth-neighbor distance [2]. When it became clear that the calculated interaction ranges exceeded those available in LAMOCA, we began development of a new code. This new code, dubbed McMOT, can deal with arbitrary interaction ranges and has the capability to model additional lattices such as T and H interstitial sites.

3.1 LAMOCA Calculations

Medium range interactions up to sixth-nearest neighbor are employed with periodic boundary conditions. Two dopants and two native point defects (vacancies and interstitials) are allowed.

The values of ν_m for interstitial and vacancy hops are chosen so that the diffusivities of isolated point defects are [11] $D_V = 1.18 \times 10^{-4} \exp(-0.1/k_B T) \text{ cm}^2\text{s}^{-1}$ and $D_I = 0.158 \exp(-1.37/k_B T) \text{ cm}^2\text{s}^{-1}$. Although these values might seem unusual in light of more recent theoretical and Watson's experimental work, we nevertheless use them in order to allow comparisons to previous work which to a large degree was based upon these values. Vacancy-vacancy and interstitial-interstitial interactions are chosen to match cluster binding energies from Jaraiz *et al.* [12].

3.2 McMOT Calculations

In order to extend the capabilities of LAMOCA, we have developed an alternative KLMC code, which has an arbitrary interaction potential. This enables us to use potentials up to the range of our *ab initio* calculations (18 shells), and to investigate the effects of truncation.

In order to investigate effects of shorter-ranged interactions, we have calculated capture radii for two alternative methods of cropping interaction potentials. One approach is to simply truncate the potential; all data for larger shell numbers than given are zero and all potential values inside the range are unchanged. A second approach is to also shift the potential; all data for larger shell numbers than given are zero and all potential values inside the range are shifted so that the potential goes

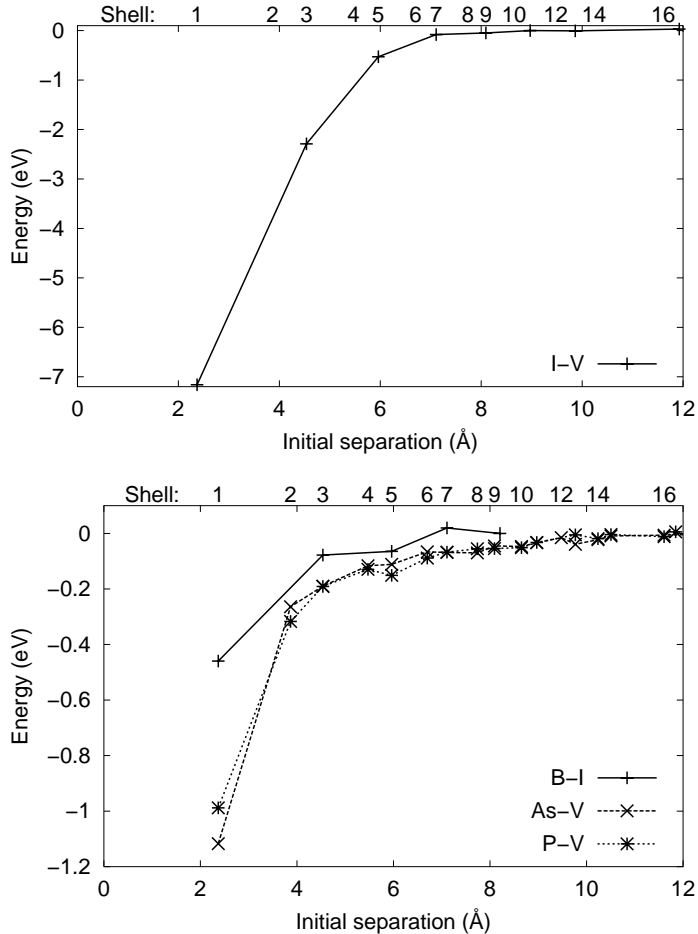


Figure 1: Calculated interaction energy as a function of separation for I-V, B-I, AS-V, and P-V. The corresponding interaction shells are also shown.

‘smoothly’ to zero – e.g., if the potential is given to be ‘6 shells (shifted)’ then the potential has been subtracted by the potential value at the 7th shell.

Simulations were conducted in a $48 \times 48 \times 48$ unit cell cube. The value of parameters such as ν_m were taken to be the same as used in LAMOCA. For the dopant-vacancy capture radii simulations shown in this paper, it was assumed that the dopant was substitutional and unable to move. We have also used this code to examine the effect of temperature on capture radii and the ‘ring mechanism’ for vacancy assisted As diffusion.

4 RESULTS

4.1 VASP

The results of the *ab initio* calculations are plotted, relative to the energy at infinite separation in Fig. 1. The *ab initio* calculations show the existence of long range interactions between defects in silicon, which extend up to at least eighth-nearest neighbors. The interactions are dependent on separation distance, but also

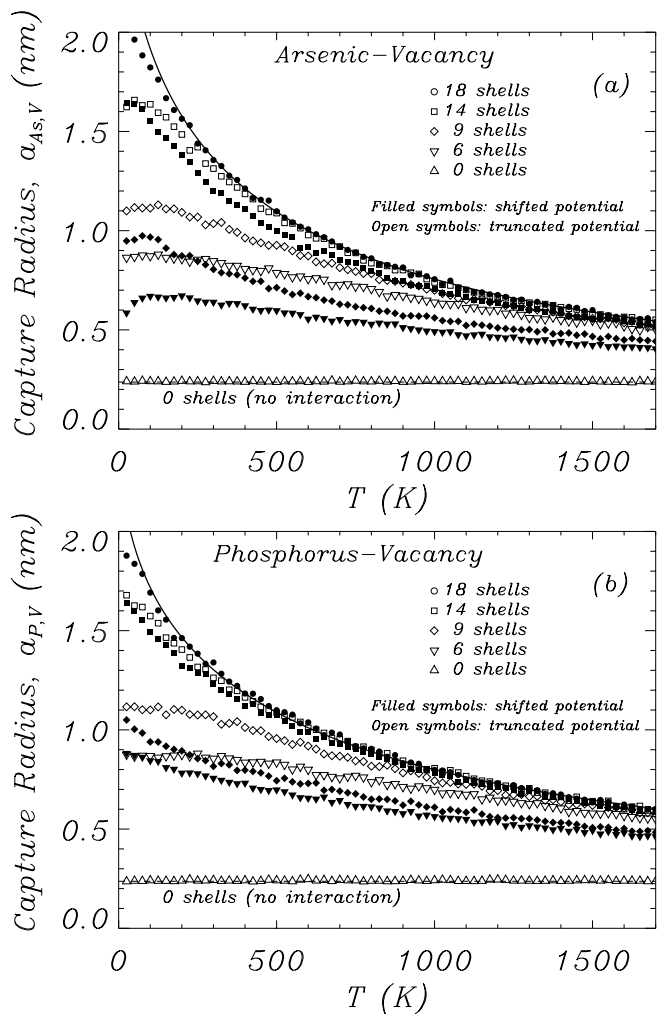


Figure 2: Calculated As-V and P-V capture radii as a function of temperature and potential truncation.

on the direction of displacement with respect to crystal orientation and the orientation of the split interstitial defects. To obtain a pair potential, the lowest energy at each distance was used. In the case of I-B and I-V interactions, the tetrahedral instead of the $\langle 110 \rangle$ split interstitial gave the lowest energy at a given separation, which results from charge transfer to the B atom or V, respectively, who both prefer the negative over the neutral charge state (see, e.g., [13]).

4.2 LAMOCA

The calculated capture radius is approximately 7 Å for I-V recombination when interactions up to sixth nearest neighbor (the maximum possible in LAMOCA) are taken into account. This is the same as previously calculated using interaction potentials obtained by empirical MD simulation [2], although the interaction potentials themselves differ significantly. Hence, it appears that the interaction range, not the shape of the potential is what determines the capture radius.

The *ab initio* results indicate an attractive potential up to the eleventh neighbor shell. We have therefore attempted to ‘trick’ LAMOCA by introducing a five neighbor offset into the tabulated potential, then adding the corresponding distance to the calculated capture radii. The interaction potential then used in LAMOCA is from sixth to eleventh neighbor rather than first to sixth. After using this offset we find a radius of 8.3 Å for I-V and 4.6 Å for B-I. All simulations were performed at 900° C.

4.3 McMot

Figure 2 shows the temperature dependence of capture radii up to 1700 K for both As-vacancy and P-vacancy. Each point represents statistics from about 80,000 capture events, each event starting with random initial lattice positions of the dopant and a vacancy, logging the time it takes for the vacancy to occupy a nearest neighbor lattice site to the dopant. The figure includes capture radii calculated using interaction potentials cropped in the two ways described above, which show considerable differences particularly for the short range interactions, where truncating induces a sharp potential well at the truncation distance.

Based on the 18 shell range potentials, the capture radii are fit very well (see solid lines fit in figure 3) in the temperature range of 300 K < T < 1700 K by $a_{x,V} = a_0 + a_1 \exp(-\sqrt{T/T_1})$, where $a_0 = 2.369$ Å is the silicon bond length. We fit $a_1 = 28.93$ Å and $T_1 = 339$ K for As-V and $a_1 = 23.15$ Å and $T_1 = 499$ K for P-V.

While these fits seem quite good, additional work needs to be conducted to verify that the 18 shell potential used in this work is indeed sufficient to characterize the capture radii.

It is found that the capture radius increases slightly as the temperature is reduced, as might be expected since at low T the capture probability increases for the weaker binding energies seen at larger distances.

We do observe the ring mechanism for vacancy assisted As diffusion, but statistical analysis of the KLMC data does not clearly support that the ring mechanism is something intrinsic to the *interaction* between two objects. Instead, it is likely just an artifact of a “random” walk on the lattice. The ring mechanism is not particularly strengthened at low temperatures (below 800 K). This can be understood by realizing that the first transition of the ring mechanism from a dopant neighbor site to a second nearest neighbor site, which all mechanisms must make, is the dominant energy transition compared to any other vacancy lattice transition. Thus, once the vacancy is no longer at a neighbor site to a dopant, minor effects of the interaction remain.

5 CONCLUSIONS

Using *ab initio* calculation and KLMC simulation, we have determined the capture radii for several defect

pairs in Si. The calculated capture radii seem far larger than those currently used in most continuum diffusion models due to the relatively long range of the interaction potential. We have also identified a temperature dependency on the capture radii for As-vacancy and P-vacancy and provided the parameterizations of the fits for temperatures above 300 K.

The close range ring mechanism for vacancy assisted substitutional dopant diffusion can appear to be very profound if one uses a truncated (un-scaled) potential with, say 4-6, neighbor shells. In that case, the potential has the form of a bowl which it is hard to exit. However, using smooth, long range interactions, the localized ring mechanism becomes less profound and seems to appear statistically, more as a result of a random walk on a lattice than as a result of the dopant-vacancy interaction.

6 ACKNOWLEDGMENTS

The KLMC computer code LAMOCA was developed at Boston University, with funding from the Semiconductor Research Corporation. We thank Marius Bunea for his invaluable assistance with the LAMOCA code. WW thanks Dr. Art Voter for very helpful discussions.

REFERENCES

- [1] M. M. Bunea, Ph.D. Thesis, Boston Univ. (2000).
- [2] Marius M. Bunea, Pavel Fastenko and Scott T. Dunham, Mat. Res. Soc. Proc. **568** p. 135.
- [3] O. Pankratov, H. Huang, T. D. de la Rubia and C. Mailhot, Phys. Rev. B, **56**, 13172 (1997).
- [4] J. S. Nelson, P. A. Schultz and A. F. Wright, Appl. Phys. Lett. **73**, 247 (1998).
- [5] J. Xie and S. P. Chen, Phys. Rev. Lett **83**, 1795 (1999); J. Phys. Cond. Matter **11**, 7219 (1999); J. Appl. Phys. **87**, 4160 (2000).
- [6] S.T. Dunham and C.D. Wu., JAP **78**, 2362 (1995).
- [7] M. Hane, T. Ikezawa, K. Takeuchi, and G. H. Gilmer, Proc. IEDM 2001.
- [8] G. Kresse and J. Hafner, Phys. Rev. B **47**, 558, (1993); *ibid.* **49**, 14251 (1994); G. Kresse and J. Furthmüller, Comput. Mat. Sci. **6**, 15 (1996); Phys. Rev. B **54**, 11169 (1996). G. Kresse and J. Hafner, J. Phys.: Condens. Matt. **6**, 8245 (1994).
- [9] M. J. Puska, S. Pöykkö, M. Pesola, and R. M. Nieminen, Phys. Rev. B **58**, 1318 (1998).
- [10] S. M. Hu, Phys. Status Solidi B **60**, 595 (1973).
- [11] M. Tang, L. Colombo, J. Zhu and T. Diaz de la Rubia, Phys. Rev B **55**, 14279, (1997).
- [12] M. Jaraiz, G. H. Gilmer and J. M. Poate, Appl. Phys. Lett. **68**, 409 (1996).
- [13] W. Windl, M. M. Bunea, R. Stumpf, S. T. Dunham, and M. P. Masquelier, Phys. Rev. Lett. **83**, 4345 (1999); in Proc. MSM 1999 (Computational Publications, Cambridge, MA 1999), p. 369.